

Supplemental information

	<i>Sequence #1</i>	<i>Sequence #2</i>	<i>Sequence #3</i>
Routine			
Number of slices	33	31	31
Distance factor	10%	10%	10%
Phase encoding direction	A>>P	A>>P	A>>P
FOV read	192 mm	200 mm	200mm
Slice thickness	4mm	4mm	4mm
TR	2000 ms	2000 ms	2000 ms
TE	30 ms	30 ms	30 ms
Contrast			
Flip angle	90 deg.	90 deg.	90 deg.
Resolution			
Base resolution	64	96	96
Phase resolution	100%	100%	100%
PAT mode	None		
Geometry			
Multi-slice mode	Interleaved	Interleaved	Interleaved
Series	Interleaved	Interleaved	Interleaved

Table SI-1: Details of the three scanning sequences.

Participant	Localizer – session 1	Localizer – session 2
7 (unique ID: 007)	<i>SNloc_ips189</i>	<i>SWJN_v1_ips252</i>
19 (unique ID: 019)	<i>SWNloc_ips168</i>	<i>SWNloc_ips168</i>
21 (unique ID: 021)	<i>SWNloc_ips168</i>	<i>SWJN_v2_ips232</i>
23 (unique ID: 023)	<i>SWNloc_ips168</i>	<i>SWJN_v2_ips232</i>
24 (unique ID: 024)	<i>SWJN_v2_ips232</i>	<i>SWJN_v2_ips232</i>
30 (unique ID: 030)	<i>SWNloc_ips168</i>	<i>SWJN_v2_ips232</i>
39 (unique ID: 040)	<i>SWNloc_ips168</i>	<i>SWNloc_ips168</i>
40 (unique ID: 041)	<i>SWNloc_ips168</i>	<i>SNloc_ips232</i>
45 (unique ID: 045)	<i>SWNloc_ips168</i>	<i>SWNloc_ips168</i>
46 (unique ID: 047)	<i>SWNloc_ips168</i>	<i>SWNloc_ips168</i>
47 (unique ID: 048)	<i>SWNloc_ips168</i>	<i>SWNloc_ips168</i>
49 (unique ID: 050)	<i>SWNloc_ips168</i>	<i>SWNloc_ips168</i>
53 (unique ID: 056)	<i>SWNloc_ips168</i>	<i>SWNloc_ips168</i>
58 (unique ID: 061)	<i>SWNloc_ips168</i>	<i>SWNloc_ips168</i>
69 (unique ID: 072)	<i>SWNloc_ips198</i>	<i>SWNloc_ips198</i>
72 (unique ID: 076)	<i>SWNloc_ips168</i>	<i>SWNloc_ips168</i>
74 (unique ID: 078)	<i>SWNloc_ips168</i>	<i>SWNloc_ips168</i>
80 (unique ID: 084)	<i>SWNloc_ips168</i>	<i>SWNloc_ips168</i>
81 (unique ID: 085)	<i>SWNloc_ips168</i>	<i>SWNloc_ips168</i>
90 (unique ID: 095)	<i>SNloc_ips189</i>	<i>SWNloc_ips168</i>
96 (unique ID: 101)	<i>SWNloc_ips168</i>	<i>SWNloc_ips168</i>
98 (unique ID: 103)	<i>SNloc_ips189</i>	<i>SWNloc_ips168</i>
107 (unique ID: 113)	<i>SNloc_ips189</i>	<i>SWNloc_ips198</i>
117 (unique ID: 123)	<i>SNloc_ips189</i>	<i>SWNloc_ips198</i>

118 (unique ID: 124)	<i>SNloc_ips189</i>	<i>SNloc_ips189</i>
120 (unique ID: 126)	<i>SNloc_ips189</i>	<i>SWNloc_ips198</i>
121 (unique ID: 127)	<i>SNloc_ips189</i>	<i>SWNloc_ips198</i>
123 (unique ID: 129)	<i>SWNloc_ips198</i>	<i>SNloc_ips189</i>
126 (unique ID: 132)	<i>SWNloc_ips198</i>	<i>SWNloc_ips198</i>
136 (unique ID: 142)	<i>SNloc_ips189</i>	<i>SNloc_ips189</i>
140 (unique ID: 146)	<i>SWNloc_ips198</i>	<i>SNloc_ips189</i>
142 (unique ID: 148)	<i>SNloc_ips189</i>	<i>SNloc_ips189</i>

Table SI-2: Information on the localizer versions for participants who were scanned across two scanning sessions.

The effects of coils and sequences

For reporting the normative distributions in Section 1, we evaluated the potential effects of coil (12- vs. 32-channel) and acquisition sequence (see Table SI-1) on the functional measures. To do so, we compared the size of the *Sentences* > *Nonwords* effect (averaging across LH regions) between participants scanned on the 12-channel coil vs. the 32-channel coil. The effect size was significantly greater for the 32-channel coil (beta-.22, $t = 3.654$, $p < 0.001$). We then added sequence to the regression and compared the model fit with and without sequence. Including sequence significantly improved the model by a likelihood ratio test ($F(2, 148) = 14.48$, $p < 0.0001$), suggesting that sequence, like coil, significantly affects the effect size measure. Other functional measures also show sensitivity to coil and sequence. Consequently, we chose to restrict our reporting to a homogeneous sample of participants scanned with the 32-channel head coil and sequence #3 (see Table SI-1).

The choice of threshold for defining individual functional ROIs

In defining the individual fROIs, we were taking the top 10% of the voxels based on the t -values for the *Sentences* > *Nonwords* contrast within each parcel. The original motivation for choosing this threshold (here and elsewhere; e.g., Blank et al., 2014, 2016; Fedorenko et al., 2015) was that it yields numbers of voxels comparable to the numbers that emerge as significant at the $p < 0.001$ uncorrected whole-brain level. Here, we evaluated the reliability of the effect size and effect-size-based lateralization measures when using a more liberal threshold (top 25% of voxels within each parcel). As expected given the use of a less selective subset of the voxels, correlations were lower overall: .63 for the effect size in the LH, .55 for the effect size in the RH, .63 for lateralization. For the lateralization measure, all 8 ROIs show an across-session correlation significantly different from 0 at $p < .05$. However, only 3/8 LH regions and 2/8 RH regions show significant correlations (Fig. SI-1 and SI-2).

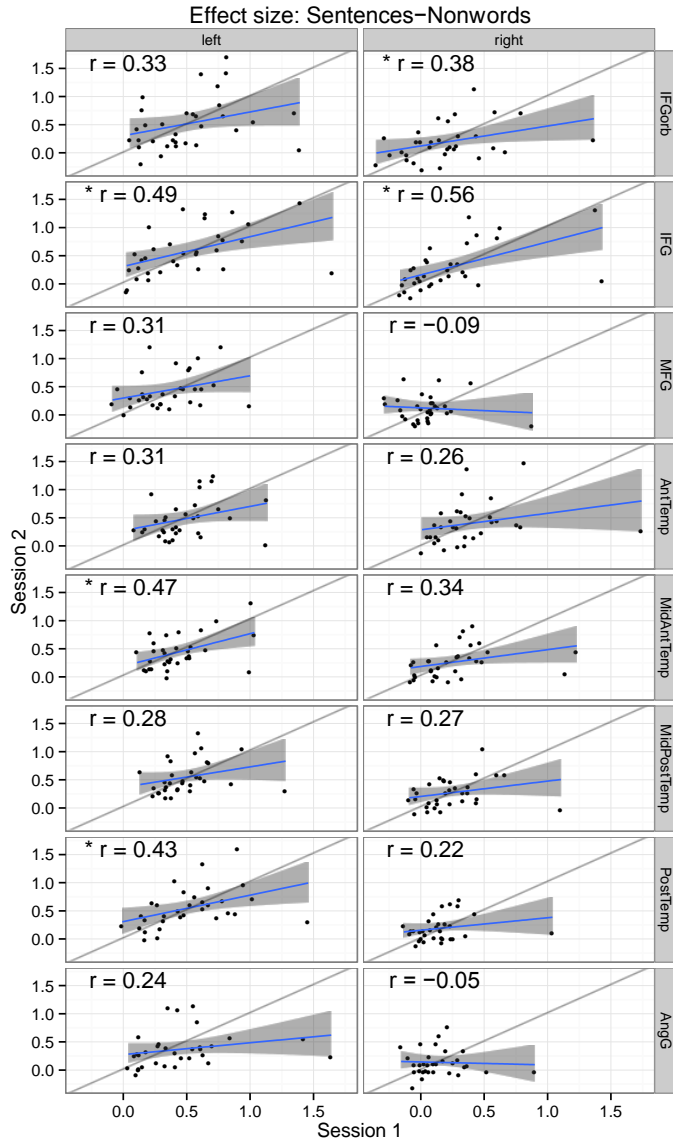


Figure SI-1: The reliability of the *Sentences > Nonwords* effect size measure in a subset of 32 participants scanned across two sessions. Unlike in the main analysis, individual fROIs are defined by taking the top 25% (cf. 10%) of the voxels within each parcel. An asterisk before the r -value indicates (uncorrected) statistical significance ($p < 0.05$).

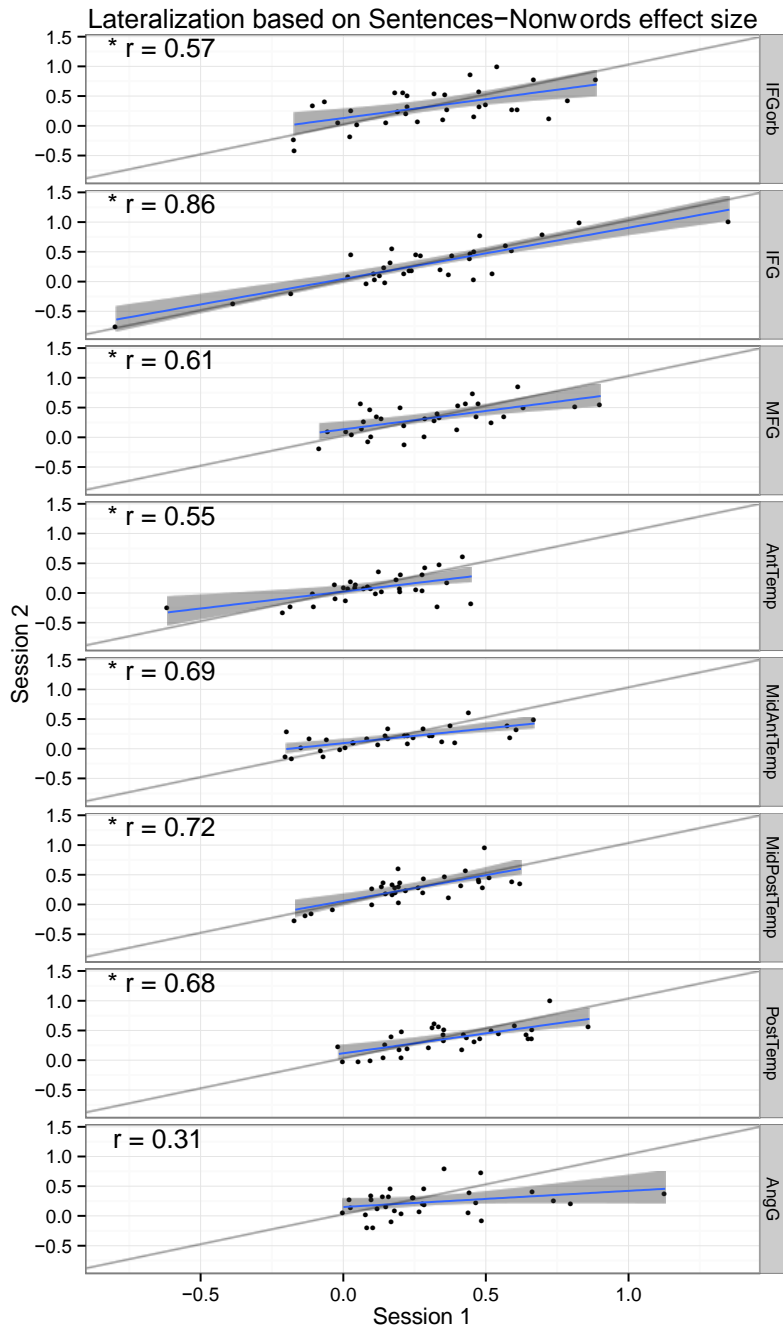


Figure SI-2: The reliability of the lateralization by effect size measure in a subset of 32 participants scanned across two sessions. Unlike in the main analysis, individual FROIs are defined by taking the top 25% (cf. 10%) of the voxels within each parcel. An asterisk before the r -value indicates (uncorrected) statistical significance ($p < 0.05$).